JOURNAL OF HARD TISSUE BIOLOGY
ISSN / eISSN 1341-7649
Publisher JOURNAL HARD TISSUE BIOLOGY,
JAPANESE RED CROSS SOCIETY, 3- 24- 20,
NISHIAZABU, MINATO KU,JAPAN, TOKYO, 106-0031
Volume 26-Issue 1-(2026)
DOI:https://doi.org/10.65281/703866

OPEN ACCESS

SIRT3 promotes tumorgenesis through deacetylation of FOXM1 and activation of mitophagy in bladder cancer cells

Check for updates

Fanlong Meng [1,2] #, Yiyang Ma [1,2] #, Meiqi Xu [1] #, Mengyuan Wu [1], Feng Pei [1,2], Haoyan Tan [3], Wenchao Shi [4], Lu Wang [1] *, Yakun Luo [1] *

1. NHC Key Laboratory of Molecular Probes and Targeted Diagnosis and Therapy, The Fourth Affiliated Hospital of Harbin Medical University, Harbin Medical University, Harbin 150081 China;
2. School of Medicine, The Fourth Affiliated Hospital of Harbin Medical University, Harbin 150001 China;
3. Department of Ultrasound, Harbin Medical University Cancer Hospital, Harbin 150080, People's Republic of China;
4. Department of Respiration, The Fourth Affiliated Hospital of Harbin Medical University, Harbin Medical University, Harbin 150001, China.

# These authors contributed equally to this work.
* Corresponding author:
Dr. Yakun Luo, E-mail: luoyankun@hrbmu.edu.cn
No. 157 Baojian Road, Harbin 150081, China
Dr. Lu Wang, E-mail: wanglu@hrbmu.edu.cn
No. 37 Yiyuan Street, Harbin 150001, China

Abstract

Bladder cancer (BLCA) remains a clinically challenging malignancy due to its high recurrence rate and frequent development of cisplatin resistance. This study reveals that SIRT3, a mitochondrial deacetylase, is significantly upregulated in BLCA tissues, and its elevated expression correlates with poor patient prognosis. Using a combination of in vitro and in vivo functional assays, we demonstrate that SIRT3 enhances BLCA cell proliferation, invasion, and migration. Mechanistically, SIRT3 directly interacts with and deacetylates the transcription factor FOXM1, leading to activation of mitophagy, as indicated by altered expression of key autophagy-related proteins such as Beclin-1, LC3B, and p62. Importantly, combined inhibition of SIRT3 (with 3-TYP) and autophagy (with chloroquine, CQ) synergistically suppresses tumor growth in both cellular and mouse xenograft models, with no significant toxicity observed. Our results identify the novel SIRT3/FOXM1/mitophagy axis as a critical driver of BLCA progression, and propose a promising therapeutic strategy for BLCA.

Keywords: SIRT3, FOXM1, mitophagy, bladder cancer, therapeutic strategy.

1. Introduction

Bladder carcinoma (BLCA) is a type of malignant tumor that originates from the mucosal lining of the urinary bladder, and globally it stands among the ten most common malignant diseases; when referring to 2022 worldwide epidemiological figures, this condition brings about roughly 614,000 new cases every year and causes around 220,000 deaths on an annual basis[1,2], with BLCA having obvious characteristics including strong invasiveness, frequent recurrence, and easy dissemination to other body parts. In terms of clinical classification, approximately 70% to 75% of BLCA cases fall into the category of non-muscle-invasive bladder cancer (NMIBC), while the remaining 25% to 30% are either muscle-invasive bladder cancer (MIBC) or metastatic bladder cancer (mBCa)[3]; for NMIBC, the current standard treatment is transurethral resection of the bladder tumor (TURBT) combined with intravesical chemotherapy, but a notable problem exists—between 17% and 45% of patients, particularly those with high-grade tumor lesions, will experience disease progression, and their condition will develop into MIBC within a five-year period. For patients with MIBC, the common treatment method is radical cystectomy combined with pelvic lymph node dissection, yet there is a limitation here: tiny metastases may already be present in the body before surgery, and this factor keeps the objective response rate at a low level, specifically ranging from 20% to 40%, in addition to which half of these patients will have their cancer spread again within three years after undergoing the operation[4-7]. Preoperative platinum-based neoadjuvant chemotherapy (NAC) is capable of targeting these hidden tiny metastases, and this treatment not only helps to enhance the effectiveness of the overall therapy but also increases the remission rates[8]; since the late 1980s, cisplatin-based systemic chemotherapy has been extensively utilized, and it still remains the core treatment for metastatic BLCA[9], while later-developed platinum-containing agents such as carboplatin and oxaliplatin have similar tumor-fighting effects and are less toxic to the human body-even so, cisplatin still holds its position as the standard treatment drug[10-12]. Clinical data reveals that cisplatin can lead to cancer remission in about 35% of

patients with metastatic BLCA[13], but there is a major issue: most patients who initially show a good response to this treatment will lose their responsiveness over time, and this is a key factor resulting in poor treatment outcomes, so it is of great importance to gain a deeper understanding of how BLCA develops, especially focusing on the molecular causes behind drug resistance, as doing so will contribute to improving the treatment strategies for BLCA.

Autophagy refers to a self-degradation process that has been retained during the course of evolution. To start with, cells enclose portions of their cytoplasm into specific structures known as autophagosomes. After that, these autophagosomes are broken down with the help of lysosomes[14]. This system acts as an important “cleaner” inside cells. It eliminates proteins that have incorrect folding or form clumps, and it also gets rid of organelles that are damaged-such as mitochondria, endoplasmic reticulum, and peroxisomes. In addition to this, it clears away pathogens that enter the interior of cells[15]. Mitophagy is a specialized kind of autophagy, and it exerts a critical function in maintaining the stable state of cells. It also assists cells in making adjustments when they encounter stress[16]. A growing number of research studies show that mitophagy has a significant impact on the initiation and development of cancer[17,18]. When talking about BLCA, unusual mitophagy activity has close connections to multiple aspects of tumor cells: the way they use energy (which is called metabolism), the speed at which they multiply, their ability to survive, and their capacity to resist drugs[19]. As an example, if mitophagy is disturbed, it may lead to issues related to metabolism. These metabolism-related problems can then promote tumor cells to multiply and maintain their survival[20]. Meanwhile, changes in mitophagy are also associated with how responsive BLCA cells are to chemotherapy drugs[21]. If we are able to fully grasp the function of mitophagy in BLCA, this could establish a key theoretical foundation for developing new methods to treat this disease.

SIRT3 is a NAD^+-dependent deacetylase that has been preserved over evolution, and it is mostly found in the mitochondria within the cytoplasm, with a small quantity also present in the cell nucleus; this enzyme alters the deacetylation of numerous substrate proteins, and by doing so, it influences a variety of biological processes-these

processes include cellular energy use (known as metabolism), the repair of DNA, the control of the cell cycle, and the process of cell death (called apoptosis)[22-24]. FOXM1 is a member of the forkhead box (FOX) family of transcription factors, and it acts as a key regulator in the initiation and growth of malignant tumors, while also having important effects on three aspects: the regulation of cell apoptosis, the response to antioxidant stress, and the changes that occur in the cell cycle[25-27]. Changes in the expression levels of SIRT3 and FOXM1, along with changes in their functional activity, are closely connected to the occurrence, development, and spread of various types of cancer[28,29], but there is a lack of full understanding-specifically, what exact roles these two proteins play and how they are regulated in BLCA have not been completely clarified yet. So, conducting research on the roles of SIRT3 and FOXM1 in BLCA is very significant, as it helps to explain the pathogenic mechanisms of this malignancy and also promotes the development of better new therapeutic strategies for treating it.

The current study is set to study two main things: first, what roles SIRT3 and FOXM1 play in BLCA, and second, how these two proteins interact with each other; it will also look at how SIRT3 and FOXM1 affect mitophagy and the way BLCA resists drugs. To do this work, the research uses three types of approaches-cellular experimental tests, animal model systems, and bioinformatics analysis methods-and through these tools, it explains the molecular ways that SIRT3 and FOXM1 make BLCA start and grow. The study's results show that SIRT3 and FOXM1 change two key abilities of BLCA cells: how they multiply, how they move, and how they resist drugs, and they do this by controlling the processes of mitophagy. This research also checks if SIRT3 and FOXM1 can be used as targets for treatment, and in doing so, it builds a theoretical base to help create new treatment plans for BLCA. People expect the findings of this research to do several things: it will make BLCA's prevention, diagnosis, and treatment better, and it will also provide more useful strategies to solve the clinical problems that come with drug resistance in BLCA patients.

2. Materials and Methods

2.1 Bioinformatics analysis

The expression of SIRT3 in BLCA tissues and the adjacent normal tissues (tissues next to BLCA tissues) was analyzed using the UALCAN online platform, with the platform's website being https://ualcan.path.uab.edu/. The relationship between SIRT3 and FOXM1 was also investigated, and this investigation was carried out via the GEPIA database; the website of this database is http://gepia.cancer-pku.cn/.

2.2 Tissue samples

BLCA tissues were collected from the Fourth Hospital of Harbin Medical University. These tissues include two types: cisplatin-resistant tumor tissues (n=19), BLCA tissues (n=30) and adjacent tissues (n=20). All tissue samples were stored in liquid nitrogen, and this storage was done to prepare for later analysis. Information about the patients was taken from medical records; this information includes the patients' age, sex, pathological stage, and T-stage. In addition, the study got approval from the institutional ethics committee (2021-WZYSLLSC-31).

2.3 Cell culture

SV-HUC-1 (normal urothelial) and BLCA lines UMUC3, EJ, 5637, RT112, T24 came from ATCC. Cells used McCoy's 5A (T24), RPMI-1640 (SV-HUC-1, 5637, EJ, RT112), or MEM (UMUC3) media (all Invitrogen, Carlsbad, CA, USA). All contained 10% FBS (Invitrogen, Thermo Fisher Scientific, Inc.) and 1% penicillin-streptomycin (Invitrogen, Carlsbad, CA, USA). Cultures grew at 37°C, 5% CO_2 with bi-monthly PCR Mycoplasma testing. BLCA cell models (T24 parental, 5637) underwent genetic manipulation to investigate SIRT3 and FOXM1 functions. Lipofectamine 2000 (Invitrogen, USA) transfected GENECHEM (Shanghai, China) plasmids. These plasmids of sh-SIRT3-#1, sh-SIRT3-#2 or OE-SIRT3 were designed and sythesised by Marjorbio (Shanghai, China). The lentivirus systems for FOXM1 knockdown (sh-FOXM1) and overexpression (OE-FOXM1) were puchased from Fenghbio (Chahngsha, China).

2.4 RNA sequencing assay

Total RNA was isolated from cell samples using TRIzol reagent, which is manufactured by Invitrogen (USA), and the concentration of the isolated RNA was measured with a NanoDrop 2000 spectrophotometer—this instrument is produced by Thermo Fisher Scientific (USA). RNA sequencing was conducted by Sangon Biotech, a biotech company based in Shanghai, China; after this sequencing step, gene expression profiles were generated with featureCounts (version v2.0.1). Differentially expressed genes (abbreviated as DEGs) were identified via DESeq2 (version v1.24.0), and the thresholds used to select these DEGs were set as follows: FDR < 0.05 and $|\log_2 FC| > 1.5$. Functional enrichment analysis was performed on the significant DEGs, and this analysis utilized both the clusterProfiler package and org.Hs.eg.db annotations. To determine the key KEGG and GO pathways, two criteria were established: a p-value of less than 0.05 and an FDR of 0.25 or lower, and this process helped to highlight the core biological pathways involved.

2.5 Western blotting assay

Cells were lysed in RIPA buffer (supplied by Solarbio), and this buffer was mixed with protease inhibitors (from Solarbio) and PMSF (also provided by Solarbio); after that, centrifugation was performed at 13,500 × g for 15 min at 4°C, and once centrifugation was completed, the protein concentration in the supernatant was measured using a BCA assay kit (supplied by Beyotime). Samples were first denatured at 95°C for 10 min, then separated via SDS-PAGE, and after separation, they were transferred onto nitrocellulose membranes-these membranes were blocked with 5% skimmed milk for 2h at room temperature. The primary antibodies used in the experiment included SIRT3 antibody (dilution 1:1000, cat. no. ab217319, Abcam, USA), Beclin-1 antibody (dilution 1:1000, cat. no. ab62557, Abcam, USA), SQSTM1/p62 antibody (dilution 1:1000, cat. no. ab207305, Abcam, USA), LC3B antibody (dilution 1:1000, cat. no. #3868, CST, USA), FOXM1 antibody (dilution 1:1000, cat. no. ab207298, Abcam, USA). β-actin antibody (dilution 1:5000, cat. no. ab8226, Abcam, USA) and GAPDH antibody (dilution 1:10000, cat. no. ab181602, Abcam, USA), were used as loading

controls. Next, the membranes were incubated with an HRP-conjugated rabbit IgG secondary antibody (dilution 1:10000, cat. no. ab205718, Abcam, USA) for 2h at room temperature, signals from the membranes were detected using ECL (supplied by Sigma-Aldrich, Inc.), and the grayscale values of these signals were quantified with ImageJ 9.0 software.

2.6 Reverse transcription quantitative PCR assay (RT-qPCR)

Cellular RNA was separated from cells using TRIzol reagent, which is produced by Invitrogen (USA). After that, a spectrophotometer was used to check two things about the extracted RNA: its purity and its concentration. When making cDNA, the ReverTra Ace kit was applied, and this kit is from Toyobo (Japan). At the same time, RT-qPCR was carried out. The tool for this step was a LightCycler 480 instrument (made by Roche), and it was used together with SsoAdvanced SYBR Green Supermix—this supermix is supplied by Bio-Rad (USA). The relative level of SIRT3 expression was calculated using the $2^{-\Delta\Delta Ct}$ method. For this calculation, ACTB was used as the reference gene to normalize the data. SIRT3 primers: forward:TCCCAGATGCTCTCTCAAGCCCGTC; reverse: GCCCAATGTCACTCACTACTTCCTG; ACTB primers: forward:AGCCATGTACGTAGCCATCC; reverse:GCTGTGGTGAAGCTGTA. All the data in this part came from three separate experimental repeats, each done independently.

2.7 Cell Counting Kit-8 (CCK-8) assay

The CCK-8 assay was used to measure how cells multiply and how harmful drugs are to them; first, cells were treated with trypsin, spun in a centrifuge, and then mixed back into complete medium, after which they were placed into 96-well plates with 2×10^3 cells in 100 μL of medium per well, and for each group and each time point (0, 24, 48, 72, 96h), five wells were prepared, while the outer wells of the plate were filled with PBS to cut down on edge effects caused by liquid drying up. The marked plates were kept in an incubator at 37°C with 5% CO_2, and at each scheduled time, 10 μL of CCK-

8 (from Beyotime) was added to each well, taking care with the pipette to avoid making bubbles, then the plates were left in the incubator for 2h at 37°C before the absorbance at 450nm was measured.

2.8 Transwell assay

Transwell assay was used to check how cells move and invade in lab settings. Matrigel that has been thawed is watered down to 1 mg/mL with serum-free medium kept on ice, and then it is mixed well. Small portions of 60 μL each are used to evenly cover the bottom surfaces of Transwell membranes. The coated chambers (made by Corning Inc., Corning, NY, USA) are left to set for 4h at 37°C. After pouring off the liquid, the upper parts of the chambers get 100 μL of serum-free medium, and they are left to soak for 30 min at 37°C. The lower parts of the chambers have 600 μL of complete medium with serum added, and this acts as a chemoattractant. Cell suspensions-with 2×10^4 cells in each chamber-are put into the upper parts. After the cells have been incubated, the chambers are taken out and the medium is sucked away. Cells that haven't moved and any leftover matrix are wiped off with damp swabs. The cells that have moved to the bottom surfaces of the membranes are fixed in 4% paraformaldehyde for 30 min at room temperature, and then they are rinsed three times with PBS. The fixed cells are stained with crystal violet for 10 min, and after that, they are washed three times with PBS. The chambers are left to dry in the air, then pictures are taken using an inverted microscope (Olympus, Tokyo, Japan). For each chamber, three random areas are recorded to count the cells and analyze the numbers.

2.9 Wound healing assay

Scratch assay was used to check how well tumor cells can move. Cells were placed in 6-well plates, with 5×10^5 cells in each well. When the cells grew to cover the whole well, uniform scratches were made using pipette tips. PBS was used to wash away any small pieces, and then the old medium was replaced with serum-free medium. Pictures were taken using phase-contrast microscopy at two times: 0h and 24h. The rate at which the scratches closed up was measured using ImageJ software.

2.10 Transmission Electron Microscope assay (TEM)

Cells that were scraped from the surface were preserved using a solution containing glutaraldehyde and osmium tetroxide. Next, these cells were dried out step by step using ethanol with different concentrations getting stronger each time, and after this drying process, they were placed into a solid medium for embedding. The embedded samples were sliced into thin sections with an ultramicrotome (produced by Leica, Germany). These thin slices were then dyed using uranyl acetate and lead citrate. In the end, the autophagosomes in the samples were looked at and pictures were taken with a transmission electron microscope (made by Hitachi, Japan).

2.11 Reactive Oxygen Species (ROS) detection assay

DCFH-DA (2',7'-Dichlorodihydrofluorescein diacetate) is a cell-penetrating substance that first gets changed by esterases through deacetylation, then gets oxidized by ROS, turning into DCF which gives off fluorescence; the strength of the light it emits at 530 nm is directly tied to how much ROS is present inside cells. Cells grown in 6-well plates had spread to cover 50-70% of each well before starting the test, and after removing the medium, these cells were put into a 10 μmol/L DCFH-DA working solution-this solution was made by mixing the original DCFH-DA (from Meilun) with serum-free medium in a 1:1000 ratio-and left at 37°C for 30 min in the dark. After this time, the samples were washed three times with serum-free medium that had been warmed up beforehand to clear away any leftover probe outside the cells, and right after these washes, fluorescence images were taken and the brightness was measured using a laser confocal microscope (from Germany).

2.12 Assessment of lysosome and mitochondria colocalization

Post-adhesion cells underwent sequential organelle staining: mitochondrial labeling with 100 nM Mito-Tracker Green (37°C, 20 min) (Beyotime), lysosomal staining with 50 nM Lyso-Tracker Red (37°C, 15 min) (Beyotime), and nuclear counterstaining with DAPI (Servicebio). Lysosome-mitochondria co-localization coefficients were

quantified using ImageJ software.

2.13 Co-immunoprecipitation assay (Co-IP)

The Co-IP test was done with a Co-IP Kit (from Beyotime). To put it simply, BLCA cells were broken down while on ice. The liquid on top (supernatant) was mixed with SIRT3 antibody (dilution 1:1000, cat. no. ab246522, Abcam, USA), FOXM1 antibody (dilution 1:1000, cat. no. ab207298, Abcam, USA), or Rabbit IgG (dilution 1:1000, cat. no. ab172730, Abcam, USA). This mix was spun slowly at 4℃ all night long. Then, Protein A/G was added, and the mix was spun at 4℃ for 3h. At the end, the supernatants were checked with western blotting.

2.14 Double Immunofluorescence (IF) staining

This method shows where two target antigens are located in the same biological samples using antibodies joined to light-emitting molecules that give off different colors of light; with two-channel fluorescence imaging, it allows for measuring protein expression levels and checking if proteins are in the same place at the same time while they are in their original position. Cells were put on coverslips that had been ready beforehand and left to attach, and after they attached, the cells were washed three times with PBS and fixed in 4% paraformaldehyde for 10 min, then after three more PBS washes, blocking was done for 60 min at room temperature, and once blocking finished, the cells were washed again with PBS three times. Next, the cells were incubated with diluted primary antibodies all night-these primary antibodies used were SIRT3 antibody (dilution 1:1000, cat. no. ab217319, Abcam, USA) and FOXM1 antibody (dilution 1:1000, cat. no. ab207298, Abcam, USA)—and this incubation happened in a damp container to stop them from drying out. After that, the cells were washed with PBS for 30 min with changes every 5 min, then incubated with a fluorescent secondary antibody for 1h with protection from light, followed by a final PBS wash for 30 min, and then the cells were stained with DAPI (from Servicebio) for 5 min; the coverslips were mounted with glycerol and pictures were taken using a Zeiss confocal microscope.

2.15 SIRT3 activity assay

SIRT3's enzyme activity was tested with the assay kit (cat. ab156067, Abcam), following the maker's directions closely. Each microplate well got 25 μL HPLC water, 5 μL SIRT3 detection buffer, 5 μL fluorescent substrate peptide, 5 μL NAD, and then 5 μL sample. At 24.0 ± 2.0 ℃, 5 μL developing reagent was added to each well to start the reaction, and the mixture was stirred thoroughly. A microplate fluorometer (SpectraMax M3, USA) measured fluorescence, with excitation at 360 nm and emission at 485 nm; readings were taken every 2 min over 60 min. This assay checked how well SIRT3 works in BLCA cells and helped explain its part in mitophagy and drug resistance[30].

2.16 Cell colony formation assay

Colony formation tests were used to see how SIRT3 and FOXM1 affect cell growth ability and cisplatin sensitivity when given different treatments. Cells were placed in 6-well plates, with 5×10^2 cells in each well. They were left to grow for 10 days at 37℃ in an environment with 5% CO_2. After that, the cells were fixed in 4% PFA for 15 min and then stained with 0.2% crystal violet (from Beyotime) for 10 min. Once they had been washed three times with PBS, groups of cells (with 50 or more cells each) were counted as living cell clusters.

2.17 GFP-LC3B plasmid transfection

Transfected cells were seeded onto culture slides and incubated at 37℃ for 24h to achieve complete adhesion. Post-adhesion, GFP-LC3 plasmid (pCMV-GFP-LC3B, D2815, Beyotime, China) transfection proceeded per manufacturer's protocol. Nuclei were subsequently counterstained with DAPI (Servicebio).

2.18 Immunohistochemistry (IHC)

Tissues were first fixed in 4% formalin and then embedded in paraffin; after that, these paraffin-embedded tissues were cut into sections, and the sections went through steps to remove paraffin and add moisture. Next, the sections were blocked with 10% goat

serum at room temperature, and this blocking step lasted for 2h. When blocking was done, the sections were incubated with primary antibodies all night long, and this incubation was carried out at 4°C. The primary antibodies used in this process included five types: SIRT3 antibody (dilution 1:500, cat. no. ab229958, Abcam, USA), FOXM1 antibody (dilution 1:1000, cat. no. ab207298, Abcam, USA), LC3B antibody (dilution 1:1000, cat. no. #3868, CST, USA), p62 antibody (dilution 1:500, cat. no. ab207305, Abcam, USA), and Ki67 antibody (dilution 1:500, cat. no. ab15580, Abcam, USA). For the step of treating with secondary antibody, an HRP-conjugated rabbit IgG antibody (dilution 1:500, cat. no. ab6721, Abcam, USA) was used for incubation. After this incubation, the next step was to develop the sections, and streptavidin-HRP was used for this development process. At last, the sections were stained again with hematoxylin, and the results of the staining were both observed and scanned using a molecular microscope (made by Olympus, Tokyo, Japan).

2.19 Hematoxylin and Eosin staining (HE)

Tissues that had been fixed with 4% formalin and embedded in paraffin were cut into sections first. Then, the sections had wax removed and got moisture added back. Next, the slices were stained with hematoxylin (from Baso), and the time for this staining was changed based on what the experiment needed. After that, the sections were rinsed with water, and then they were stained with eosin (also from Baso). Once eosin staining was done, the sections went through differentiation, dehydration with ethanol solutions of different strengths, clearing with xylene, and mounting with neutral resin. Finally, the changes in the tissue's shape and structure were observed, and pictures were taken using a microscope (made by Olympus, Tokyo, Japan).

2.20 Xenograft model

Cells that had been pretreated were put in 50 μL of McCoy's 5A medium first, and then mixed with Matrigel in a 1:1 ratio (the Matrigel was from Corning, USA). Next, 100 μL portions of this mixture were injected under the skin (subcutaneously) into both sides of the belly of male nude mice-these mice were 4 to 6 weeks old. After that, the

volume of the tumors was checked every week, and calipers were used to take the measurements. On the 28th day after the cells were inoculated, the mice were put to death. Then, the tumors were cut out from the mice, and their wet weight was recorded right away. The protocols for this experiment were approved by the Animal Ethics Committee of Harbin Medical University (approval number to be filled in), and all steps followed international guidelines.

2.21 Statistical analysis

Data following a normal distribution were expressed as mean ± standard deviation. One-way analysis of variance (ANOVA) was applied for comparisons among multiple groups, while t-tests were used for comparisons between two groups. A P-value less than 0.05 was considered to indicate statistical significance.

3. Results

3.1 SIRT3 is upregulated and linked to poor prognosis in BLCA

A thorough review of clinical data and experimental results (Fig. 1A) showed SIRT3 expression was far higher in BLCA tissues than in adjacent non-tumor tissues, with one key point being that SIRT3 levels rose gradually as BLCA progressed (Fig. 1B)-this suggests SIRT3 may promote disease development and progression. Also, RT-qPCR and western blotting were used to assess SIRT3 expression at both transcriptional and protein levels, with representative data showing SIRT3 had increased in BLCA tissues and CDDP-resistant BLCA tissues compared to adjacent normal tissues, and the increase was more significant in CDDP-resistant samples (Fig. 1C-D). IHC analysis on clinical specimens also confirmed these findings, as SIRT3 protein levels were higher in BLCA tissues than in adjacent normal tissues and even more elevated in CDDP-resistant tissues than in primary tumor tissues, with representative images shown in Fig. 1E-F. Besides, SIRT3 expression in BLCA cell lines was investigated too, and comparison with the normal bladder epithelial cell line SV-HUC-1 revealed increased SIRT3 in multiple BLCA cell lines at both mRNA and protein levels-with the highest

expression in T24 and 5637 cells, which were thus selected for subsequent validation experiments (Fig. 1G-H).

To find out what role SIRT3 plays in BLCA tumor growth, we first set up T24 cells with stable sh-SIRT3 expression-the cell line was bought from Fenghbio. These cells were used for subcutaneous xenograft models in nude mice. Then, after 4 weeks, the tumors were cut out. Both the size and weight of the tumors in the sh-SIRT3 group were much smaller than those in the control group (Fig. 1I-K). IHC staining found that Ki67 expression had gone down in the sh-SIRT3 group (Fig. 1L). This shows that sh-SIRT3 effectively stopped the tumor-forming ability and growth of BLCA cells inside the body. To sum up, these results showed that SIRT3 expression is very abnormal in BLCA, and it is closely linked to disease progression and bad clinical results. Functional experiments also proved that SIRT3 helps BLCA cells grow, which points out that it might be a possible prognostic biomarker and treatment target for BLCA.

3.2 Oncogenic role of SIRT3 in BLCA cells

To find out what function SIRT3 has in BLCA progression, we first set up BLCA cell lines-some with stable SIRT3 silencing (sh-SIRT3-#1 and sh-SIRT3-#1, from Fenghbio) and others with SIRT3 overexpression (OE-SIRT3, from Fenghbio). Then, we used Western blotting analysis to check how well SIRT3 was silenced or overexpressed, and the results are shown in Fig. 2A. We also did functional tests like CCK-8, Transwell invasion, and wound healing assays. These tests showed that sh-SIRT3 greatly stopped cell growth and the ability to invade, while OE-SIRT3 clearly made these cancer-related traits stronger (Fig. 2B-D). All these findings together show that SIRT3 pushes BLCA to progress by making cell proliferation and invasion better, which means it has tumor-promoting traits.

3.3 Role of SIRT3 in regulating mitophagy in BLCA cells

To keep finding out how SIRT3 promotes BLCA development, we first carried out RNA-seq tests on T24 cells-including those with normal SIRT3, and sh-SIRT3 (Fig.

3A)-then used the Kyoto Encyclopedia of Genes and Genomes, commonly referred to as KEGG, for enrichment analysis, which identified the autophagic pathway, mTOR pathway, and FOXO family as key factors influencing SIRT3's biological functions (Fig. 3B); guided by this analysis, we then looked into SIRT3's role in regulating mitophagy in BLCA cells, knocking out SIRT3 in T24 and 5637 cell lines and using TEM to examine mitochondrial ultrastructure, with results showing that loss of SIRT3 greatly increased mitochondrial damage and caused structural abnormalities in autophagosomes and mitochondria (Fig. 3C). At the molecular level, BECN1 (also known as Beclin-1) is a core component of the class III phosphatidylinositol 3-kinase (PI3K) complex-also called PI3KC3-and this molecule triggers the process of autophagosome formation by helping generate phosphatidylinositol-3-phosphate (PI3P)[31]; meanwhile, microtubule-associated protein 1 light chain 3 (MAP1LC3/LC3) is a critical marker for autophagosome assembly[32], using its lipidated form (LC3) to support the expansion of autophagic membranes, while the adaptor protein sequestosome 1 (SQSTM1/p62) regulates autophagic flux by linking LC3 to ubiquitinated targets, with its expression negatively correlated with autophagic activity[33]. Western blotting showed that compared to sh-Ctrl, cells with SIRT3 knocked down (sh-SIRT3) had significantly reduced levels of Beclin-1 and LC3B proteins and a notable rise in SQSTM1/p62 expression (Fig. 3D); ROS immunofluorescence staining found that loss of SIRT3 led to a sharp surge in ROS and increased cell apoptosis (Fig. 3E); also, we performed mitochondria-lysosome co-localization assays (using Mitotracker and Lysotracker), which showed that losing SIRT3 markedly reduced the overlap between mitochondria and autolysosomes (Fig. 3F)-indicating impaired mitophagic processes. All these observations together show that SIRT3 controls mitophagy in BLCA cells by regulating key autophagic molecules and maintaining mitochondrial integrity, which in turn promotes BLCA progression.

3.4 SIRT3 promotes BLCA progression via deacetylating FOXM1

To learn more about SIRT3's regulatory network, we did differential gene expression analysis on cells where sh-SIRT3 worked well, and like what's in Fig. 4A, after

knocking out SIRT3, the expression of many genes changed a lot when compared to the control group-one thing to note is that FOXM1 expression went down especially obviously, which caught our attention, and FOXM1 is well known to act as a key transcription factor when many cancers get worse, while clinical test data (Fig. 4B) also prove that FOXM1 expression is much higher in BLCA tissues than in nearby non-tumor tissues, so putting these findings together, we guess that FOXM1 might be an important downstream effector molecule of SIRT3. To check if this guess is right, we did bioinformatics checks on the BLCA cohort using the GEPIA database (Fig. 4C), and the results clearly showed a strong positive link between SIRT3 and FOXM1 mRNA expression levels, which gave more support to our experimental observations, while co-IP experiments also proved they have a direct physical connection-providing solid evidence of their molecular link (Fig. 4D)-and dual immunofluorescence staining showed that SIRT3 is in both the cytoplasm and nucleus of 5637 and T24 cells, while FOXM1 is mainly in the nucleus, and the merged fluorescence images showed clear co-localization signals around the nucleus, further proving they are close in space and might work together (Fig. 4E). To make clear the regulatory relationship between these two molecules, we knocked down or overexpressed SIRT3 in T24 and 5634 cell lines, and Western blotting tests showed that FOXM1 protein levels went down or up as expected (Fig. 4F), while specifically knocking down FOXM1 didn't affect SIRT3 expression much (Fig. 4G)-this means FOXM1 is a downstream target controlled by SIRT3-and to find out if SIRT3 controls FOXM1 through its own deacetylase activity, we used 3-TYP (3-(1H-1,2,3-triazol-4-yl) pyridine), a specific SIRT3 inhibitor, with dimethyl sulfoxide (DMSO) as the vehicle control, and this inhibitor works by binding to SIRT3's catalytic domain in a competitive way, stopping it from interacting with substrate proteins and the cofactor NAD^+, and specifically stops deacetylase activity without affecting SIRT3 protein levels[34]. Western blotting tests and fluorescence-based activity measurements showed that, compared to empty vector controls (OE-Ctrl+DMSO), OE-SIRT3 made deacetylase activity much stronger in T24 and 5637 cells, while treating with 3-TYP not only reduced the body's own SIRT3 activity but also completely blocked the activity increase caused by OE-SIRT3-proving its

inhibitory effect doesn't depend on SIRT3 expression levels (Fig. 4H)-and further studies showed that stopping SIRT3 activity made FOXM1 expression go down a lot, even with OE-SIRT3, FOXM1 still went down significantly because 3-TYP stopped deacetylase activity (Fig. 4I), so all these results together give direct evidence of how SIRT3 controls FOXM1 through deacetylation, and this gives new ideas about how BLCA develops.

3.5 SIRT3 promotes malignant progression of BLCA cells via mediating FOXM1 deacetylation

To make clear the biological role of this regulatory axis, we set up a cellular model in T24 and 5637 cells-these cells either had both OE-SIRT3 and sh-FOXM1 or carried sh-SIRT3 and OE-FOXM1 simultaneously. Then, we did CCK-8 proliferation assays, and these assays showed that sh-FOXM1 completely wiped out the promoting effect of OE-SIRT3 on cell viability and growth ability (Fig. 5A). Conversely, OE-FOXM1 fully abrogated the inhibitory effect of sh-SIRT3 on cell viability and proliferation (Fig. 5B). Colony formation experiments also proved that sh-FOXM1 greatly stopped the increased colony-forming ability caused by OE-SIRT3 (Fig. 5C). We also did Transwell invasion assays and wound-healing migration tests, and these tests showed that sh-FOXM1 effectively blocked the invasive and migratory traits triggered by OE-SIRT3 (Fig. 5D-E). All these findings from different tests together confirm that FOXM1 acts as a key downstream middle molecule for SIRT3's tumor-promoting activity.

3.6 SIRT3 induces mitophagy via FOXM1 deacetylation

To confirm that SIRT3 controls mitophagy by regulating FOXM1, we did immunofluorescence staining experiments-these experiments showed that sh-FOXM1 turned back the increase in GFP-LC3B levels caused by OE-SIRT3 (Fig. 6A). We also did Western blotting analyses, and these analyses revealed that sh-FOXM1 wiped out the regulatory effect of OE-SIRT3 on LC3B and p62 levels in BLCA cells (Fig. 6B). And besides that, we did co-localization assays using mitochondrial (Mitotracker) and lysosomal (Lysotracker) tracers (Fig. 6C), and these assays showed that sh-FOXM1

reduced the co-localization of mitochondria and autophagosomes in BLCA cells with SIRT3 overexpressed-this then made mitophagy activity go down. All these findings further confirm that SIRT3 makes mitophagy stronger in BLCA cells by deacetylating FOXM1, and this process in turn promotes cell growth, proliferation, migration, and invasion.

3.7 Effects and mechanism verification of combined intervention with SIRT3 inhibitor and autophagy inhibitor on BLCA

To keep checking the molecular mechanism-where OE-SIRT3 in BLCA starts mitophagy by deacetylating FOXM1, which then stops cancer cell death and speeds up malignant tumor growth—we designed a grouped intervention method; for in vitro lab-cell experiments, we divided BLCA cells into 4 groups: the control group (treated with DMSO), the group with SIRT3-specific inhibitor (3-TYP, 10 μM), the group with autophagy inhibitor (CQ, 10 μM), and the combination treatment group (3-TYP+CQ, 10 μM of 3-TYP plus 10 μM of CQ). First, we did CCK-8 cell viability assays, and these assays showed that compared with the control group, both the 3-TYP group and CQ group had much lower growth activity, while the combination group had an even stronger effect on stopping growth, which shows that stopping SIRT3 and blocking autophagy work together to stop BLCA cell growth (Fig. 7A). Then, Western blotting further showed that 3-TYP-by specifically blocking SIRT3's deacetylase activity-made FOXM1 expression drop a lot, and at the same time, CQ weakened the activation of mitophagy-related pathways by blocking autophagolyso-somes, which also made FOXM1 protein levels go down, with the combination group having the biggest drop in FOXM1 (Fig. 7B), and these findings proved that the SIRT3-FOXM1-mitophagy axis plays a key role in controlling BLCA cell behaviors at the molecular level. To check if this mechanism works in living organisms (in vivo), we set up a subcutaneous xenograft model in nude mice using T24 cells; when the average tumor volume reached 100 mm^3, we started giving daily belly injections: DMSO, 3-TYP (50 mg/kg), CQ (25 mg/kg), or 3-TYP+CQ (50 mg/kg of 3-TYP plus 25 mg/kg of CQ), and we measured the tumor volume every week, and after 4 weeks of non-stop intervention, we saw big

differences in tumor growth-the 3-TYP group had an average tumor volume of (500.00 ± 43.01) mm^3, the CQ group (542.00 ± 40.82) mm^3, both much smaller than the control group's (722.00 ± 41.57) mm^3, while the combination group's tumors got even smaller, down to (276.00 ± 56.28) mm^3, and this was statistically different from the groups that got only one drug (Fig. 7C). After we cut out the tumors, we weighed them and checked their shape, and the 3-TYP+CQ group had much lighter tumors (Fig. 7D-E)-this matched the volume results and proved that the combined intervention strongly stops tumor growth in living mice. Immunohistochemical staining showed key changes in protein expression in tumor tissues: compared with the control group, the 3-TYP group had no big change in SIRT3 expression (which matches that 3-TYP only stops SIRT3's activity, not its amount), the CQ group had a small drop in SIRT3, and both groups had lower FOXM1 and LC3B levels plus higher p62 levels-these changes were most obvious in the combination group (Fig. 7F), which shows that stopping SIRT3 and blocking autophagy work together to stop FOXM1-mediated mitophagy. Also, during the experiment, the mice didn't have unusual weight changes, and pathological sections of major organs (heart, liver, lung, kidney) showed no toxic damage, which proves that giving 3-TYP and CQ together is well-tolerated in living mice (Fig. 7G). All these findings—from lab cells and living mice-confirm that OE-SIRT3 in BLCA cells promotes tumor growth and malignant progression by turning on FOXM1-mediated mitophagy, but using 3-TYP+CQ together specifically blocks this pathway and greatly stops cell growth; this discovery not only gives direct evidence that the SIRT3-FOXM1-mitophagy axis affects BLCA progression but also provides a possible combined treatment plan to deal with clinical problems like treatment resistance.

4. Discussion

BLCA remains a clinically intractable malignancy. Cisplatin resistance stands as a critical barrier to improving patient prognosis. Only around 35% of patients with metastatic disease attain remission via cisplatin-based chemotherapy. Most of these patients eventually develop refractory disease[35]. SIRT3 is a mitochondria-enriched

deacetylase. FOXM1 is a pro-oncogenic transcription factor. Both molecules have been individually confirmed to correlate with cancer progression[36,37]. However, their regulatory interaction in cisplatin-resistant BLCA has long been unclear. This is especially true for the regulatory role mediated through the mitophagy pathway. To address this unmet research need, this study combined bioinformatic mining approaches, in vitro cellular assays, and in vivo xenograft experiments. It systematically analyzed the SIRT3-FOXM1-mitophagy axis. The key findings of the study are as follows. First, SIRT3 is upregulated in BLCA tissues. Its expression is more prominent in cisplatin-resistant samples. Moreover, SIRT3 expression correlates with poor prognosis. Second, SIRT3 exerts oncogenic effects. These effects promote the proliferation, invasion, and cisplatin resistance of BLCA cells. Third, SIRT3 can deacetylate FOXM1. It also regulates the expression of Beclin-1, LC3B, and p62. Through these actions, SIRT3 activates mitophagy. Finally, combined inhibition of SIRT3 and autophagy can synergistically suppress BLCA growth. The inhibitor 3-TYP is used to target SIRT3. CQ is used to inhibit autophagy. This combined treatment shows favorable tolerability both in vitro and in vivo.

When viewed against existing literature, this study′s findings align with recent research outcomes regarding SIRT3′s oncogenic role. Some research has demonstrated that SIRT3 drives pancreatic cancer development through mitochondrial regulation[38]. Other studies have linked FOXM1 to colorectal cancer progression[39]. All these studies echo the data on the pro-tumor effects of the SIRT3-FOXM1 axis in BLCA observed in this research. Meanwhile, the association between mitophagy and cisplatin resistance in BLCA revealed here is also consistent with relevant research results. That research showed METTL3 can activate the BNIP3-independent Pink1-Parkin mitophagy pathway via the m6A-DCP2 axis. This activation ultimately induces chemoresistance[40]. It is noteworthy that in previous studies, SIRT3-mediated deacetylation was often considered a regulatory mechanism for inhibiting gene expression. For example, one study found that in pancreatic cancer cells, SIRT3 can compress the chromatin conformation of the HIF-1α gene promoter. It achieves this

by deacetylating histone H3K9. This process ultimately downregulates HIF-1α expression. In turn, it blocks epithelial-mesenchymal transition[41]. However, in specific cancers, SIRT3-mediated deacetylation can also promote gene expression. One study confirmed this in hepatocellular carcinoma. In this context, SIRT3 can enhance the kinase activity of GSK-3β through deacetylation. This enhancement activates the BAX gene promoter. It further upregulates BAX expression. Through this dual mechanism, SIRT3 initiates the apoptotic pathway[42]. Essentially, this functional difference is an adaptive response of SIRT3. It responds to the specific substrates and metabolic demands of different tumors. The substrates in question are histone H3K9/HIF-1α versus GSK-3β/BAX. The metabolic demands include hypoxic metabolic adaptation in pancreatic cancer and apoptotic regulation under energy stress in hepatocellular carcinoma.

The core innovation of this study is the revelation of a non-metabolic regulatory mechanism. This mechanism underlies the role of the SIRT3-FOXM1-mitophagy axis in BLCA progression and cisplatin resistance. This finding provides new insights into the field. SIRT3 is a deacetylase primarily localized in mitochondria. Numerous studies have reported that SIRT3 affects tumorigenesis in various cancers. It does this by regulating metabolic processes. For example, one study found that SIRT3 regulates mitophagy in triple-negative breast cancer. It achieves this by acetylating the metabolic enzyme pyruvate dehydrogenase (PDH)[43]. Although the regulatory relationship between SIRT3 and certain transcription factors (such as FOXO3) has been extensively studied, its interaction with FOXM1 in BLCA has not been identified before. This study is the first to propose a key mechanism in BLCA. In this setting, SIRT3 activates mitophagy not by directly targeting metabolic enzymes. Instead, it does so through deacetylation modification of the transcription factor FOXM1. This activation ultimately promotes the proliferation, invasion, and cisplatin resistance of tumor cells. This finding not only expands the understanding of SIRT3′s mechanism of action in cancer. It also provides a new perspective for understanding the non-metabolic

regulatory pathway of mitophagy in BLCA. Furthermore, it fills the research gap in the mechanism of cisplatin resistance in this field.

Despite the progress mentioned above, this study still has several limitations that can be further addressed. First, the specific acetylation site of FOXM1 targeted by SIRT3 remains unclear. One study has confirmed that the post-translational modification sites of FOXM1 are associated with its oncogenic activity[44]. This study has initially verified the interaction between SIRT3 and FOXM1. It has also verified their regulatory effect on mitophagy. However, clarifying the specific modification site in subsequent studies will enable a more in-depth analysis of the underlying mechanism. Second, no correlation analysis has been conducted between the activity of the SIRT3-FOXM1-mitophagy axis and clinical cisplatin response. Clinical cisplatin response includes indicators such as progression-free survival. This type of analysis will provide additional evidence for the association between the axis′s function and clinical efficacy. Currently, the conclusions of this study focus on the basic mechanism level. Integrating clinical sample data in subsequent research can further enhance its reference value for translational studies.

To address the aforementioned limitations and expand the value of this research, future studies can advance in three aspects. Firstly, researchers can combine liquid chromatography-tandem mass spectrometry (LC-MS/MS) with site-directed mutagenesis experiments. This combination will allow accurate identification of the specific acetylation site of FOXM1 targeted by SIRT3. It will lay a molecular foundation for deciphering the regulatory mechanism between the two molecules. Second, researchers can include more than 200 pairs of cisplatin-sensitive/resistant BLCA samples from clinical cohorts. They can detect the expression levels of SIRT3, FOXM1, and mitophagy markers (LC3B, p62) via immunohistochemistry. Then, they can use Cox regression models to analyze the association between these indicators and clinical outcomes. Clinical outcomes include progression-free survival and overall survival. This analysis will provide clinical evidence support for mechanism research. Thirdly, researchers can use single-cell RNA sequencing technology. They can explore

whether the combined use of the SIRT3 inhibitor 3-TYP and the autophagy inhibitor CQ exerts regulatory effects on other pathways. These pathways include the PI3K/Akt/mTOR pathway. They can also investigate whether this combination affects the function of immune cells in the tumor microenvironment (TME). Such effects include changes in PD-L1 expression. This exploration will further expand the potential value of combined therapy.

Overall, this study holds significant translational value. At the mechanistic level, it confirms that SIRT3 regulates mitophagy through the transcription factor FOXM1 rather than metabolic enzymes. This confirmation expands the scope of understanding regarding SIRT3′s role in cancer. It also addresses the limitation of previous studies that focused solely on SIRT3′s metabolic function. At the therapeutic level, this study provides proof-of-concept for the combined inhibition of SIRT3 and autophagy. Based on this, the proposed 3-TYP+CQ regimen offers a promising targeted alternative strategy. It is designed for cisplatin-resistant BLCA, a disease with currently limited treatment options. At the prognostic level, the study identifies SIRT3 and FOXM1 as biomarkers. These biomarkers can be used to stratify high-risk patients with cisplatin-resistant BLCA. This stratification supports the early adjustment of treatment strategies. In summary, the SIRT3-FOXM1-mitophagy axis serves as a novel therapeutic target and biomarker panel for cisplatin-resistant BLCA. It lays a solid foundation for the clinical translation of targeted mitophagy inhibition. It also highlights the importance of conducting subsequent multi-center studies and preclinical validations.

5. Conclusion

Our study reveals that SIRT3 promotes bladder cancer progression and cisplatin resistance by deacetylating FOXM1 to activate mitophagy, and targeting this pathway may offer new therapeutic strategies.

Ethics approval and consent to participate

The study was conducted in accordance with the Declaration of Helsinki, and approved by the Ethics Committee of the Fourth Affiliated Hospital of Harbin Medical University (protocol code 2021-WZYSLLSC-31 and Nov. 14th, 2022). All animal experiments were performed in compliance with the National Institutes of Health Guide for the Care and Use of Laboratory animals (NIH Publication no. 8023, amended 1978) and described in compliance with the ARRIVE guidelines.

Authors' contributions

FM: Investigation, Methodology; MX and MW: Validation. FP and HT: Formal analysis, Methodology, Validation. YL: Resources, Conceptualization, Funding acquisition, Project administration, Writing – original draft.

Acknowledgements

We are grateful to Dr Zhichong Wu for scientific and technical input.

Funding

This work was supported by the National Natural Science Foundation of China (No. 82503606), the Natural Science Foundation of Heilongjiang Province, China (No. YQ2023H015), the Research Fund of the Fourth Affiliated Hospital of Harbin Medical University (No. HYDSYRCYJ02).

Availability of data and materials

All data generated in the present study may be requested from the corresponding author.

Conflicts of Interest

The authors declare no conflict of interest.

Patient consent for publication

Not applicable.

Reference

[1] Goutas D, Tzortzis A, Gakiopoulou H, Vlachodimitropoulos D, Giannopoulou I, Lazaris AC. Contemporary Molecular Classification of Urinary Bladder Cancer. In Vivo. 2021 Jan-Feb;35(1):75-80.

[2] Bray F, Laversanne M, Sung H, Ferlay J, Siegel RL, Soerjomataram I, Jemal A. Global cancer statistics 2022: GLOBOCAN estimates of incidence and mortality worldwide for 36 cancers in 185 countries. CA Cancer J Clin. 2024 May-Jun;74(3):229-263.

[3] Shih KW, Chen WC, Chang CH, Tai TE, Wu JC, Huang AC, Liu MC. Non-Muscular Invasive Bladder Cancer: Re-envisioning Therapeutic Journey from Traditional to Regenerative Interventions. Aging Dis. 2021 Jun 1;12(3):868-885.

[4] Miyagi H, Kwenda E, Ramnaraign BH, Chatzkel JA, Brisbane WG, O'Malley P, Crispen PL. Predicting Complete Response to Neoadjuvant Chemotherapy in Muscle-Invasive Bladder Cancer. Cancers (Basel). 2022 Dec 28;15(1):168.

[5] Felsenstein KM, Theodorescu D. Precision medicine for urothelial bladder cancer: update on tumour genomics and immunotherapy. Nat Rev Urol. 2018 Feb;15(2):92-111.

[6] Sylvester RJ, van der Meijden AP, Oosterlinck W, Witjes JA, Bouffioux C, Denis L, Newling DW, Kurth K. Predicting recurrence and progression in individual patients with stage Ta T1 bladder cancer using EORTC risk tables: a combined analysis of 2596 patients from seven EORTC trials. Eur Urol. 2006 Mar;49(3):466-5; discussion 475-7.

[7] Li F, Zheng Z, Chen W, Li D, Zhang H, Zhu Y, Mo Q, Zhao X, Fan Q, Deng F, Han C, Tan W. Regulation of cisplatin resistance in bladder cancer by epigenetic mechanisms. Drug Resist Updat. 2023 May;68:100938.

[8] Advanced Bladder Cancer (ABC) Meta-analysis Collaboration. Neoadjuvant chemotherapy in invasive bladder cancer: update of a systematic review and meta-analysis of individual patient data advanced bladder cancer (ABC) meta-analysis collaboration. Eur Urol. 2005 Aug;48(2):202-5; discussion 205-6.

[9] Sternberg CN, de Mulder PH, Schornagel JH, Théodore C, Fossa SD, van Oosterom AT, Witjes F, Spina M, van Groeningen CJ, de Balincourt C, Collette L; European Organization for Research and Treatment of Cancer Genitourinary Tract Cancer Cooperative Group. Randomized phase III trial of high-dose-intensity methotrexate, vinblastine, doxorubicin, and cisplatin (MVAC) chemotherapy and recombinant human granulocyte colony-stimulating factor versus classic MVAC in advanced urothelial tract tumors: European Organization for Research and Treatment of Cancer Protocol no. 30924. J Clin Oncol. 2001 May 15;19(10):2638-46.

[10] Zhang C, Xu C, Gao X, Yao Q. Platinum-based drugs for cancer therapy and anti-tumor strategies. Theranostics. 2022 Feb 7;12(5):2115-2132.

[11] McQuade RM, Stojanovska V, Bornstein JC, Nurgali K. PARP inhibition in platinum-based chemotherapy: Chemopotentiation and neuroprotection. Pharmacol Res. 2018 Nov;137:104-113.

[12] Zhou J, Kang Y, Chen L, Wang H, Liu J, Zeng S, Yu L. The Drug-Resistance Mechanisms of Five Platinum-Based Antitumor Agents. Front Pharmacol. 2020 Mar 20;11:343.

[13] von der Maase H, Hansen SW, Roberts JT, Dogliotti L, Oliver T, Moore MJ, Bodrogi I, Albers P, Knuth A, Lippert CM, Kerbrat P, Sanchez Rovira P, Wersall P, Cleall SP, Roychowdhury DF, Tomlin I, Visseren-Grul CM, Conte PF. Gemcitabine and cisplatin versus methotrexate, vinblastine, doxorubicin, and cisplatin in advanced or metastatic bladder cancer: results of a large, randomized, multinational, multicenter, phase III study. J Clin Oncol. 2000 Sep;18(17):3068-77.

[14] Noda NN, Inagaki F. Mechanisms of Autophagy. Annu Rev Biophys. 2015;44:101-22.

[15] Kaushik S, Cuervo AM. The coming of age of chaperone-mediated autophagy. Nat Rev Mol Cell Biol. 2018 Jun;19(6):365-381.

[16] Onishi M, Yamano K, Sato M, Matsuda N, Okamoto K. Molecular mechanisms and physiological functions of mitophagy. EMBO J. 2021 Feb 1;40(3):e104705.

[17] Xu HM, Hu F. The role of autophagy and mitophagy in cancers. Arch Physiol Biochem. 2022 Apr;128(2):281-289.

[18] Panigrahi DP, Praharaj PP, Bhol CS, Mahapatra KK, Patra S, Behera BP, Mishra SR, Bhutia SK. The emerging, multifaceted role of mitophagy in cancer and cancer therapeutics. Semin Cancer Biol. 2020 Nov;66:45-58.

[19] Li D, Su H, Deng X, Huang Y, Wang Z, Zhang J, Chen C, Zheng Z, Wang Q, Zhao S, Chen ZS, Chen H, Hou L, Tan W, Li F. DARS2 Promotes Bladder Cancer Progression by Enhancing PINK1-Mediated Mitophagy. Int J Biol Sci. 2025 Jan 27;21(4):1530-1544.

[20] Ferro F, Servais S, Besson P, Roger S, Dumas JF, Brisson L. Autophagy and mitophagy in cancer metabolic remodelling. Semin Cell Dev Biol. 2020 Feb;98:129-138.

[21] Wu Q, Yu H, Sun H, Lv J, Zhuang J, Cai L, Jiang L, Chen Y, Tao Y, Bai K, Yang H, Yang X, Lu Q. SRSF1-mediated alternative splicing regulates bladder cancer progression and cisplatin sensitivity through HIF1A/BNIP3/mitophagy axis. J Transl Med. 2025 May 22;23(1):571.

[22] Salvatori I, Valle C, Ferri A, Carrì MT. SIRT3 and mitochondrial metabolism in neurodegenerative diseases. Neurochem Int. 2017 Oct;109:184-192.

[23] Jin J, Bai L, Wang D, Ding W, Cao Z, Yan P, Li Y, Xi L, Wang Y, Zheng X, Wei H, Ding C, Wang Y. SIRT3-dependent delactylation of cyclin E2 prevents hepatocellular carcinoma growth. EMBO Rep. 2023 May 4;24(5):e56052.

[24] Xu K, He Y, Moqbel SAA, Zhou X, Wu L, Bao J. SIRT3 ameliorates osteoarthritis via regulating chondrocyte autophagy and apoptosis through the PI3K/Akt/mTOR pathway. Int J Biol Macromol. 2021 Apr 1;175:351-360.

[25] Ghosh S, Singh R, Vanwinkle ZM, Guo H, Vemula PK, Goel A, Haribabu B, Jala VR. Microbial metabolite restricts 5-fluorouracil-resistant colonic tumor

progression by sensitizing drug transporters via regulation of FOXO3-FOXM1 axis. Theranostics. 2022 Jul 18;12(12):5574-5595.

[26] Madureira PA, Varshochi R, Constantinidou D, Francis RE, Coombes RC, Yao KM, Lam EW. The Forkhead box M1 protein regulates the transcription of the estrogen receptor alpha in breast cancer cells. J Biol Chem. 2006 Sep 1;281(35):25167-76.

[27] Niinuma T, Kitajima H, Sato T, Ogawa T, Ishiguro K, Kai M, Yamamoto E, Hatanaka Y, Nojima I, Toyota M, Yorozu A, Sekiguchi S, Tohse N, Furuhashi M, Ohguro H, Miyazaki A, Suzuki H. LINC02154 promotes cell cycle and mitochondrial function in oral squamous cell carcinoma. Cancer Sci. 2025 Feb;116(2):393-405.

[28] Ouyang S, Zhang Q, Lou L, Zhu K, Li Z, Liu P, Zhang X. The Double-Edged Sword of SIRT3 in Cancer and Its Therapeutic Applications. Front Pharmacol. 2022 Apr 27;13:871560.

[29] Khan MA, Khan P, Ahmad A, Fatima M, Nasser MW. FOXM1: A small fox that makes more tracks for cancer progression and metastasis. Semin Cancer Biol. 2023 Jul;92:1-15.

[30] Liu Y, Cai X, Cai Y, Chang Y. lncRNA OIP5-AS1 Suppresses Cell Proliferation and Invasion of Endometrial Cancer by Regulating PTEN/AKT via Sponging miR-200c-3p. J Immunol Res. 2021 Jul 28;2021:4861749.

[31] Li S, Banck M, Mujtaba S, Zhou MM, Sugrue MM, Walsh MJ. p53-induced growth arrest is regulated by the mitochondrial SirT3 deacetylase. PLoS One. 2010 May 5;5(5):e10486.

[32] Li R, Quan Y, Xia W. SIRT3 inhibits prostate cancer metastasis through regulation of FOXO3A by suppressing Wnt/β-catenin pathway. Exp Cell Res. 2018 Mar 15;364(2):143-151.

[33] Battistini C, Kenny HA, Zambuto M, Nieddu V, Melocchi V, Decio A, Lo Riso P, Villa CE, Gatto A, Ghioni M, Porta FM, Testa G, Giavazzi R, Colombo N, Bianchi F, Lengyel E, Cavallaro U. Tumor microenvironment-induced FOXM1 regulates ovarian cancer stemness. Cell Death Dis. 2024 May 28;15(5):370.

[34] Gao J, Zhang K, Wang Y, Guo R, Liu H, Jia C, Sun X, Wu C, Wang W, Du J, Chen J. A machine learning-driven study indicates emodin improves cardiac hypertrophy by modulation of mitochondrial SIRT3 signaling. Pharmacol Res. 2020 May;155:104739.

[35] Dasari S, Tchounwou PB. Cisplatin in cancer therapy: molecular mechanisms of action. Eur J Pharmacol. 2014 Oct 5;740:364-78.

[36] Wu F, Wu S, Huang Y, Xiao X, Yu H, Bai X, Zhang C, Feng Z, Li L, Mei Y, Li X, Gou X. Smoking promotes the progression of bladder cancer through FOXM1/CKAP2L axis. J Transl Med. 2025 Jul 11;23(1):785.

[37] Liao M, Sun X, Zheng W, Wu M, Wang Y, Yao J, Ma Y, Gao S, Pei D. LINC00922 decoys SIRT3 to facilitate the metastasis of colorectal cancer through up-regulation the H3K27 crotonylation of ETS1 promoter. Mol Cancer. 2023 Oct 4;22(1):163.

[38] Liu LW, Xie Y, Li GQ, Zhang T, Sui YH, Zhao ZJ, Zhang YY, Yang WB, Geng XL, Xue DB, Chen H, Wang YW, Lu TQ, Shang LR, Li ZB, Li L, Sun B. Gut microbiota-derived nicotinamide mononucleotide alleviates acute pancreatitis by activating pancreatic SIRT3 signalling. Br J Pharmacol. 2023 Mar;180(5):647-666.

[39] Bian Y, Xu S, Gao Z, Ding J, Li C, Cui Z, Sun H, Li J, Pu J, Wang K. m6A modification of lncRNA ABHD11-AS1 promotes colorectal cancer progression and inhibits ferroptosis through TRIM21/IGF2BP2/ FOXM1 positive feedback loop. Cancer Lett. 2024 Aug 1;596:217004.

[40] Sun Y, Shen W, Hu S, Lyu Q, Wang Q, Wei T, Zhu W, Zhang J. METTL3 promotes chemoresistance in small cell lung cancer by inducing mitophagy. J Exp Clin Cancer Res. 2023 Mar 17;42(1):65.

[41] Zhou B, Lei JH, Wang Q, Qu TF, Cha LC, Zhan HX, Liu SL, Hu X, Sun CD, Guo WD, Qiu FB, Cao JY. Cancer-associated fibroblast-secreted miR-421 promotes pancreatic cancer by regulating the SIRT3/H3K9Ac/HIF-1α axis. Kaohsiung J Med Sci. 2022 Nov;38(11):1080-1092.

[42] Song CL, Tang H, Ran LK, Ko BC, Zhang ZZ, Chen X, Ren JH, Tao NN, Li WY, Huang AL, Chen J. Sirtuin 3 inhibits hepatocellular carcinoma growth through the glycogen synthase kinase-3β/BCL2-associated X protein-dependent apoptotic pathway. Oncogene. 2016 Feb 4;35(5):631-41.

[43] Yang H, Zhou L, Shi Q, Zhao Y, Lin H, Zhang M, Zhao S, Yang Y, Ling ZQ, Guan KL, Xiong Y, Ye D. SIRT3-dependent GOT2 acetylation status affects the malate-aspartate NADH shuttle activity and pancreatic tumor growth. EMBO J. 2015 Apr 15;34(8):1110-25.

[44] Lv C, Zhao G, Sun X, Wang P, Xie N, Luo J, Tong T. Acetylation of FOXM1 is essential for its transactivation and tumor growth stimulation. Oncotarget. 2016 Sep 13;7(37):60366-60382.

Figure legends

Figure 1. SIRT3 is upregulated and correlates with poor prognosis in BLCA. (A) SIRT3 expression profiles in BLCA tissues (n=408) compared with nearby normal tissues (n=19), data sourced from the TCGA dataset. (B) SIRT3 expression levels across different clinical stages of BLCA progression. (C-D) SIRT3 expression at transcriptional and protein levels in normal tissues, primary BLCA tissues, and CDDP-resistant BLCA tissues. (E) Western blotting showing SIRT3 protein levels in paired BLCA tissues (marked as T) and adjacent normal tissues (marked as N). (F) Western blotting comparing SIRT3 expression between primary BLCA tissues and CDDP-resistant BLCA tissues, with higher expression in CDDP-resistant ones. (G-H) Transcriptional and protein levels of SIRT3 in several BLCA cell lines compared with the normal bladder epithelial cell line SV-HUC-1. (J) Representative images of subcutaneous xenograft tumors (n=6 per group). (I-K) Growth curves and weight quantifications of xenograft tumors in the sh-SIRT3 group and sh-Ctrl group. (L) Representative Hematoxylin-Eosin (HE) staining (Scale bar = 50 μm) and Ki67 immunostaining (Scale bar = 50 μm) of xenograft tumors from the sh-SIRT3 group and

sh-Ctrl group. Statistical data are presented as mean ± standard error. For significance labels: ns denotes no significance, * stands for $P < 0.05$, ** represents $P < 0.01$, and *** signifies $P < 0.001$.

Figure 1

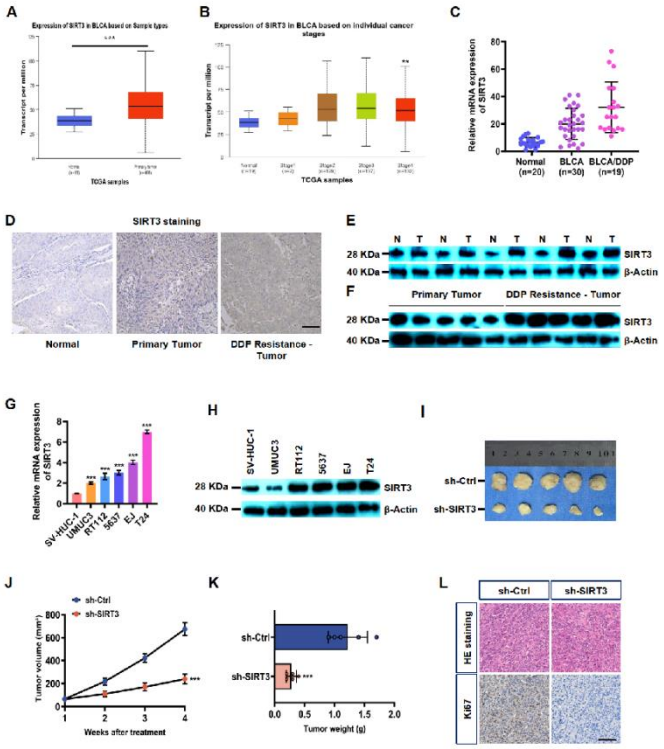

Figure 2. Oncogenic functions of SIRT3 in BLCA cells. (A) Western blotting to check how well SIRT3 was knocked down or overexpressed in BLCA cells. (B) Cell viability tests for BLCA cells with SIRT3 silenced or overexpressed. (C) Transwell invasion assays (Scale bar = 50 μm) to test the invasive ability of BLCA cells with changed SIRT3 expression. (D) Wound healing assays (Scale bar = 200 μm) to measure the migratory ability of BLCA cells with altered SIRT3. Statistical data are shown as mean ± standard error. For significance labels: ns means no significance, * stands for $P < 0.05$, ** means $P < 0.01$, and *** represents $P < 0.001$.

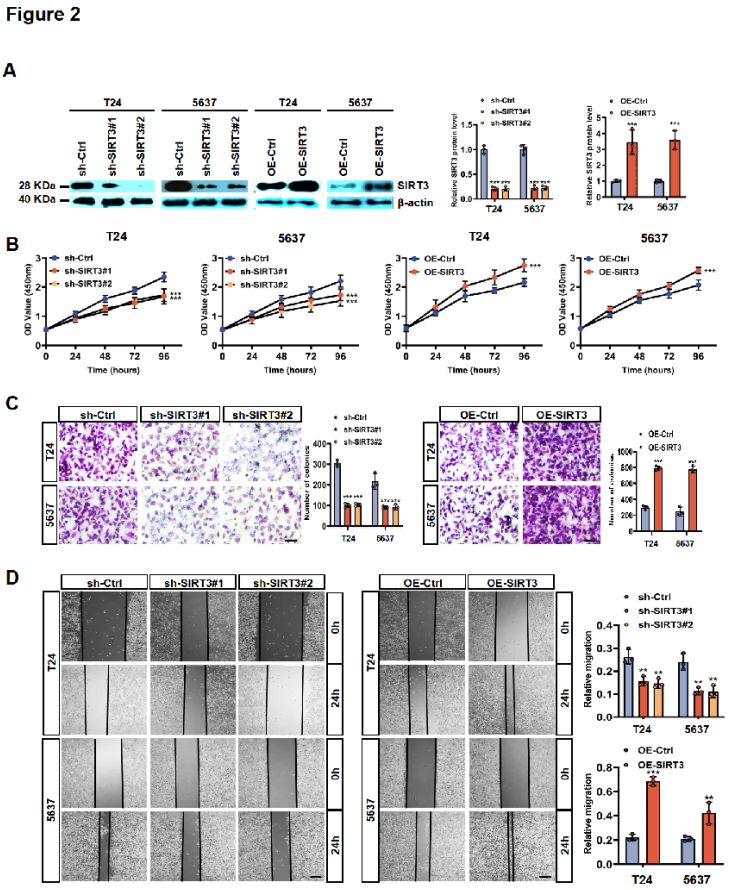

Figure 3. SIRT3 knockdown induces BLCA cell death by triggering autophagy. (A) RNA sequencing heatmap for comparing gene expression profiles between the sh-Ctrl group and sh-SIRT3 group. (B) KEGG pathway enrichment analysis of differentially expressed genes after SIRT3 knockdown. (C) TEM images (Scale bar = 10 μm) showing mitochondrial ultrastructure in BLCA cells with sh-SIRT3. (D) Western blotting analysis of Beclin-1, LC3B, and p62 expression in BLCA cells with sh-SIRT3. (E) ROS immunofluorescence staining (Scale bar = 200 μm) assessing ROS production in BLCA cells with sh-SIRT3. (F) Co-localization immunofluorescence using MitoTracker and LysoTracker (Scale bar = 50 μm) to evaluate mitophagy in BLCA cells with sh-SIRT3. Statistical data are expressed as mean ± standard error. For significance notation: ns denotes no significance, * indicates $P < 0.05$, ** represents $P < 0.01$, and *** signifies $P < 0.001$.

Figure 3

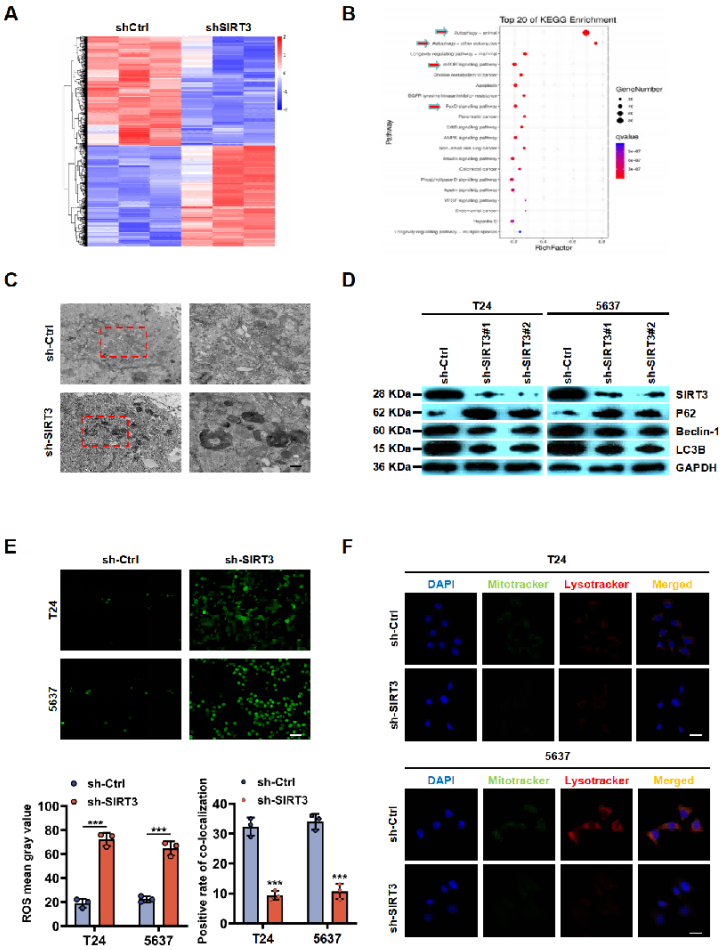

Figure 4. SIRT3 regulates FOXM1 via its deacetylase activity. (A) SIRT3 knockdown causes changes in the expression of many downstream genes, including FOXM1. (B) FOXM1 expression in BLCA tissues (n=404) compared with normal tissues (n=28), data from the TCGA dataset. (C) Correlation analysis of SIRT3 and FOXM1 expression in BLCA. (D) Co-IP verification of the SIRT3-FOXM1 protein interaction. (E) Subcellular co-localization of SIRT3 and FOXM1 (Scale bar = 50 μm) in BLCA cells. (F) FOXM1 protein expression in BLCA cells with SIRT3 knockdown or overexpression. (G) SIRT3 protein levels in BLCA cells with sh-FOXM1. (H) FOXM1 expression in BLCA cells treated with OE-SIRT3 and/or 3-TYP. (I) Detection of the effect of 3-TYP treatment on SIRT3 activity. Statistical data are expressed as mean ± standard error. For significance notation: ns denotes no significance, * indicates $P < 0.05$, ** represents $P < 0.01$, and *** signifies $P < 0.001$.

Figure 4

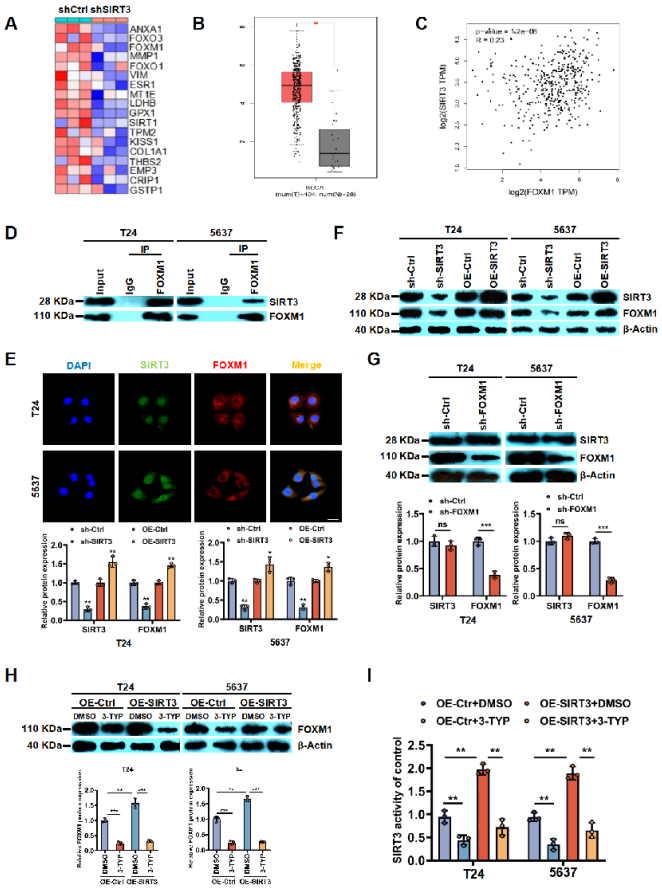

Figure 5. Functional validation of the SIRT3-FOXM1 regulatory axis in BLCA cells. (A) Viability of BLCA cells following OE-SIRT3 and sh-FOXM1 manipulation. (B) Cell viability in BLCA cells with sh-SIRT3 and OE-FOXM1 treatment. (C) Colony formation assays in BLCA cells with OE-SIRT3 and sh-FOXM1. (D) Wound healing assays (Scale bar = 200 μm) for migration in BLCA cells with OE-SIRT3 and sh-FOXM1. (E) Transwell invasion assays (Scale bar = 50 μm) for invasive capacity in BLCA cells with OE-SIRT3 and sh-FOXM1. Statistical data are expressed as mean ± standard error. For significance notation: ns denotes no significance, * indicates $P < 0.05$, ** represents $P < 0.01$, and *** signifies $P < 0.001$.

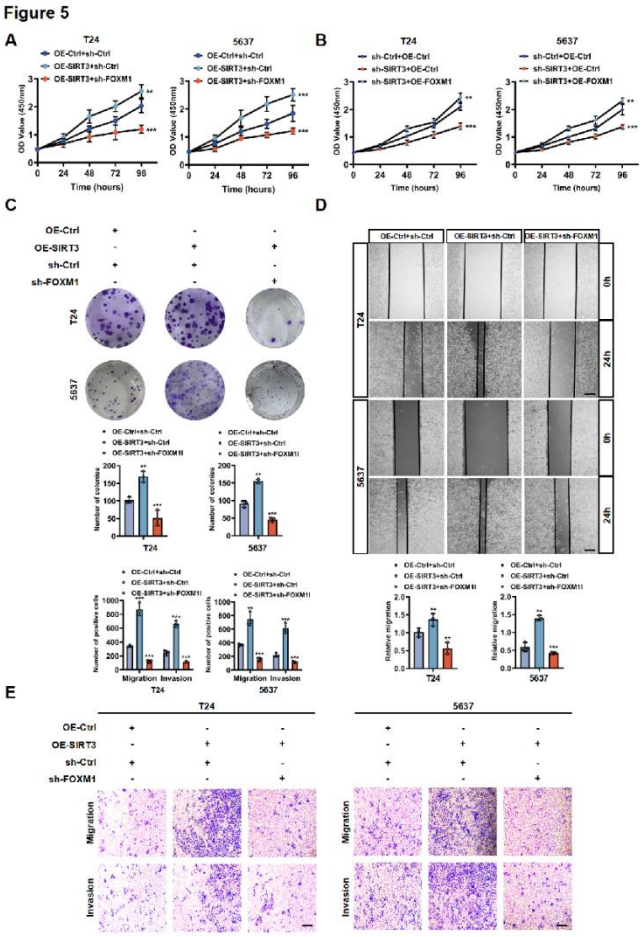

Figure 6. Impact of OE-SIRT3 on FOXM1-mediated mitophagy in BLCA cells. (A) Immunofluorescence staining (Scale bar = 50 μm) for GFP-LC3B plasmid transfection efficiency in BLCA cells under different interventions. (B) Western blotting analysis of LC3B and p62 protein levels in BLCA cells in different intervention groups. (C) Co-immunofluorescence staining with MitoTracker and LysoTracker (Scale bar = 50 μm) for mitochondrial-autophagosome co-localization in BLCA cells from different groups. Statistical data are expressed as mean ± standard error. For significance notation: ns denotes no significance, * indicates $P < 0.05$, ** represents $P < 0.01$, and *** signifies $P < 0.001$.

Figure 6

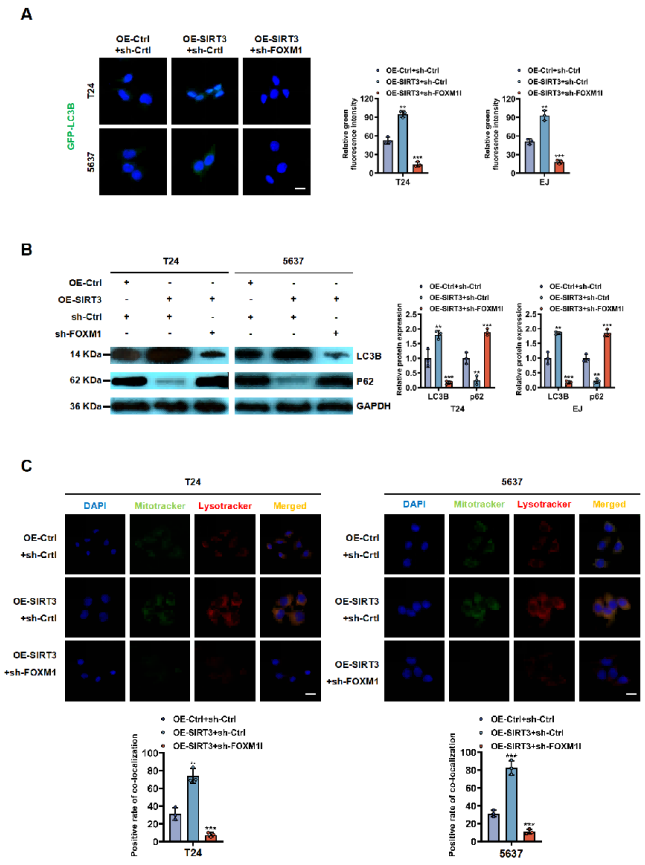

Figure 7. Intervention effects of combined SIRT3 inhibitor and autophagy inhibitor on BLCA models. BLCA cells were given DMSO (as control), SIRT3 inhibitor 3-TYP, autophagy inhibitor chloroquine (CQ), or the combination of 3-TYP and CQ. (A) Viability assays of the treated BLCA cells. (B) Western blotting analysis of SIRT3 and FOXM1 protein expression in the treated BLCA cells. (C) Subcutaneous xenograft tumor models (n=5). (D-E) Tumor volume growth curves and mouse body weight data. (F) Immunohistochemical staining of SIRT3, FOXM1, p62, and LC3B in tumor tissues (Scale bar = 50 μm, n=5). (G) HE staining of tumor tissues. Statistical data are expressed as mean ± standard error. For significance notation: ns denotes no significance, * indicates $P < 0.05$, ** represents $P < 0.01$, and *** signifies $P < 0.001$.

Figure 7

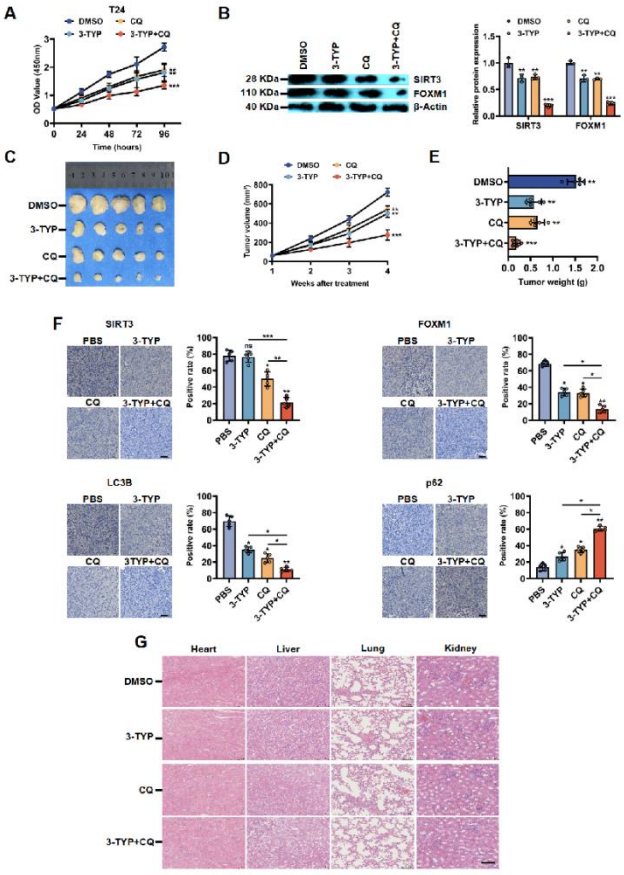
A
T24
DMSO
CQ
3-TYP
3-TYP+CQ
OD Value (450nm)
Time (hours)
B
DMSO
3-TYP
CQ
3-TYP+CQ
28 KDa
110 KDa
40 KDa
SIRT3
FOXM1
β-Actin
Relative protein expression
C
DMSO
3-TYP
CQ
3-TYP+CQ
D
Tumor volume (mm³)
Weeks after treatment
E
Tumor weight (g)
F
SIRT3
FOXM1
LC3B
p62
PBS
3-TYP
CQ
3TYP+CQ
Positive rate (%)
G
Heart
Liver
Lung
Kidney